

ANALYSIS OF MECHANICAL PROPERTIES AND ANTIBACTERIAL ACTIVITY AGAINST STAPHYLOCOCCUS AUREUS OF KNITTED FABRICS PREPARED FROM NANO-ZNO TWISTED YARNS

MING-CHUN HSIEH¹, MEI-CHEN LIN^{2*}, YAN-YU LIN^{3*}, MING- HUANG LIN⁴, JIA-HORNG LIN^{4,5*}, CHIEN-TENG HSIEH⁶, YUEH-SHENG CHEN⁷, CHING-WEN LOU^{1,8*}

¹Department of Bioinformatics and Medical Engineering, Asia University, Taichung 41354, Taiwan

²Department of Biomedical Engineering, College of Biomedical Engineering, China Medical University, Taichung 404333, Taiwan

³Department of Fashion and Accessories Design, Ling Tung University, Taichung 408213, Taiwan.

⁴Department of Fiber and Composite Materials, Feng Chia University, Taichung 40768, Taiwan

⁵School of Chinese Medicine, China Medical University, Taichung 40402, Taiwan

⁶Department of Fashion Design and Merchandising, Shih Chien University, Kaohsiung 84550, Taiwan

⁷Department of Biomedical Engineering, China Medical University, Taichung 406040, Taiwan

MEI-CHEN LIN: lmc9363@mail.cmu.edu.tw

YAN-YU LIN: yyulin@teamail.ltu.edu.tw

JIA-HORNG LIN: jhlin@fcu.edu.tw

CHING-WEN LOU: cwlou@asia.edu.tw

Corresponding Author: MEI-CHEN LIN

ABSTRACT

This study investigates the effects of the twisting process of yarns containing zinc oxide nanoparticles (ZnO NPs) on the mechanical properties and antibacterial performance of knitted fabrics, and evaluates their feasibility as functional textile materials. Two- and three-ply ZnO-containing yarns were prepared using a ring-twisting machine at various speeds to obtain twist coefficients ranging from 0 to 5. The twisted yarns were then fabricated into knitted fabrics and evaluated for their physical properties, including hairiness, tensile strength, air permeability, and water vapor transmission rate (WVTR). Results revealed that increasing the twist coefficient significantly reduced yarn hairiness, indicating enhanced fiber compactness. The fabrics with a twist coefficient of 3 (samples 2Zn-3C-K and 3Zn-3C-K) exhibited optimal mechanical strength and air permeability, whereas excessive twisting (≥ 4) led to a decrease in tensile strength due to fiber over-twisting. For antibacterial evaluation, *Staphylococcus aureus* (*S. aureus*) was used as the test strain. The results showed a marked reduction in bacterial colonies with increasing twist coefficients, achieving antibacterial rates of 87% and 90% for samples 2Zn-5C-K and 3Zn-5C-K, respectively.

KEYWORDS: Zinc oxide nanoparticles (ZnO NPs); *Staphylococcus aureus* (*S. aureus*); coefficient of twist; knitted fabrics; colony count.

1. INTRODUCTION

With the increasing awareness of personal health protection and continuous advances in textile and medical technologies, hygiene consciousness has become an integral part of daily life. The focus of textile development has gradually shifted from mere wearing comfort to multifunctional product design, particularly toward textiles with antibacterial properties [1], [2]. Because textiles remain in prolonged contact with human skin, they are easily contaminated by perspiration, sebum, and keratinized metabolites—providing a favorable environment for microbial growth. Among these microbes, *Staphylococcus aureus* (*S. aureus*), a Gram-positive bacterium commonly found on skin and in the environment, can proliferate on textile surfaces, leading to unpleasant odors, material degradation, and even skin infections or other health issues [3].

Antibacterial agents used in textiles are generally classified into three types: organic, inorganic, and natural. Although early organic agents exhibited strong antibacterial efficacy, their limited stability and durability, as well as potential toxicity, have restricted their use. In contrast, inorganic antibacterial agents are thermally stable, long-lasting, and more environmentally and

biologically compatible [4]. Silver ions possess excellent antibacterial properties but are costly, limiting large-scale applications. Zinc oxide nanoparticles (ZnO NPs), by comparison, are non-toxic, biocompatible, and recognized as “Generally Regarded As Safe” (GRAS) by the U.S. Food and Drug Administration [5], [6], [7]. Owing to these advantages, ZnO NPs have gained wide attention in antibacterial textiles, especially in medical applications, where they effectively inhibit common hospital-associated bacteria such as *S. aureus* and *Escherichia coli*, both major causes of nosocomial infections[8].

The antibacterial mechanisms of ZnO NPs include the generation of reactive oxygen species (ROS), the release of Zn²⁺ ions, and the disruption of bacterial cell wall formation[9].

Several studies have confirmed the antimicrobial efficacy of ZnO NPs against various microorganisms, including *E. coli*, *S. aureus*, and *Bacillus subtilis* [10], [11], [12]. Arputharaj et al. reported that cotton fabrics treated with ZnO NPs retained significant antibacterial activity against *S. aureus* and *Klebsiella pneumoniae* even after five washing cycles [13]. Similarly, Patil et al. [14] and Babu et al[15]. demonstrated that physically modified ZnO nanoparticles applied to cotton fabrics could substantially enhance antibacterial performance and durability, providing an effective route for textile functionalization. Furthermore, ZnO NPs are widely used in sunscreens for ultraviolet (UV) protection and in artificial tooth coatings to improve durability and biocompatibility. In environmental applications, ZnO NPs serve as catalysts or adsorbents in wastewater treatment and textile waste management, helping remove pollutants in an eco-friendly manner. Consequently, ZnO NPs represent a promising component of sustainable functional textiles [16], [17], [18].

Yarn processing methods such as coating or twisting can alter yarn structure, potentially influencing its functional performance. Studies have indicated that excessive twisting reduces yarn hygroscopicity and capillary efficiency [19], [20]. Knitted structures, owing to their superior elasticity, air permeability, and conformability, are highly valued in functional textile development. Compared with woven fabrics, knitted fabrics possess larger specific surface areas, enhancing their capacity to incorporate and activate functional materials [21], [22].

In this study, ZnO nanoparticle-containing yarns were twisted using a ring-twisting machine to produce two- and three-ply composite wrapped yarns. By adjusting the spindle speed and winding rate, yarns with different twist coefficients were obtained. These yarns were then fabricated into knitted fabrics using a fully computer-controlled single-cylinder knitting machine. The resulting fabrics were characterized for mechanical properties, water vapor transmission rate (WVTR), and air permeability. Antibacterial activity against *S. aureus* was evaluated through colony counting, optical density (OD) measurements, and inhibition rate analysis. The combined results were used to determine the optimal processing parameters for achieving balanced mechanical and antibacterial performance.

2. EXPERIMENTAL

Figure 1 illustrates the experimental procedure of this study. ZnO nanoparticle-containing yarns were first subjected to a twisting process to produce yarns with different twist coefficients. These twisted yarns were then knitted into fabrics, which were subsequently evaluated for their antibacterial performance.

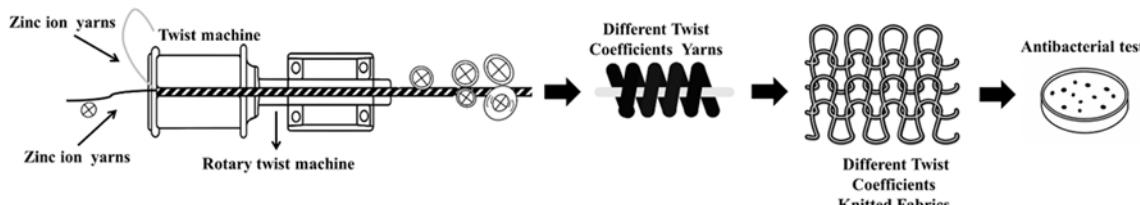


Figure 1. Schematic diagram of the experimental procedure in this study.

2.1 MATERIALS

A 30-count yarn containing nano-zinc oxide (ZnO NPs) was supplied by TUNG HO TEXTILE CO., LTD. (Taiwan). This base yarn was subjected to a twisting process to prepare 12 types of twisted yarns with varying parameters.

For the antibacterial evaluation, *Staphylococcus aureus* (S. aureus, ATCC 25923) was procured from the Bioresource Collection and Research Center (BCRC, Taiwan).

2.2 EXPERIMENTAL SAMPLE PREPARATION

The preparation of the nano-ZnO twisted yarns involved a two-step process. First, the base 30-count nano-ZnO yarns were plied into two-strand (two-ply) and three-strand (three-ply) configurations using an automatic winding machine. Subsequently, these plied yarns were twisted using a ring-twisting machine. Yarns with different twist coefficients were obtained by varying the rotational speed difference between the winding and take-up components of the machine.

A nomenclature system was established to identify the samples, as summarized in Table 1. In this system, the number preceding "Zn" (e.g., 2Zn-) indicates the number of plies (two-ply). The number preceding "C" (e.g., 3C-) represents the twist coefficient. The suffix "C" denotes the sample in its yarn state, while the suffix "K" (e.g., 2Zn-3C-K) signifies the final knitted fabric prepared from that yarn. Due to the large number of specifications in this study, samples will be referred to by this nomenclature hereafter.

Table 1. Sample nomenclature.

| ZnO | Sample codes (tested in yarn form) | Sample codes (tested in knitted fabric form) | coefficient of twist |
|-----------|------------------------------------|--|----------------------|
| Two-ply | 2Zn-0C | 2Zn-0C-K | 0 |
| | 2Zn-1C | 2Zn-1C-K | 1 |
| | 2Zn-2C | 2Zn-2C-K | 2 |
| | 2Zn-3C | 2Zn-3C-K | 3 |
| | 2Zn-4C | 2Zn-4C-K | 4 |
| | 2Zn-5C | 2Zn-5C-K | 5 |
| Three-ply | 3Zn-0C | 3Zn-0C-K | 0 |
| | 3Zn-1C | 3Zn-1C-K | 1 |
| | 3Zn-2C | 3Zn-2C-K | 2 |
| | 3Zn-3C | 3Zn-3C-K | 3 |
| | 3Zn-4C | 3Zn-4C-K | 4 |
| | 3Zn-5C | 3Zn-5C-K | 5 |

Preparation of ZnO Knitted Fabrics

Two-ply and three-ply ZnO yarns were twisted using a rotor twisting machine at different spindle speeds of 0, 3000, 6000, 9000, 12,000, and 15,000 rpm, corresponding to twist coefficients of 0, 1, 2, 3, 4, and 5, respectively. The twisted yarns were then knitted into fabrics using a fully computerized, high-efficiency, single-cylinder hosiery knitting machine (Model DK-B318, Da Kong Enterprise Co., Ltd., Taiwan). A total of twelve fabric samples with different processing parameters were prepared for subsequent experiments.

2.3 EXPERIMENTAL TESTING

2.3.1 MECHANICAL PROPERTIES OF KNITTED FABRICS

The tensile strength (breaking tenacity) of the ZnO knitted fabrics was measured according to ASTM D5034 using a universal tensile testing machine (Model HT-2402, Hung Ta Instrument Co., Ltd., Taiwan). The gauge length was set at 100 mm, and the crosshead speed at 300 mm/min. Each specimen measured 20 cm × 2.5 cm, and ten tests were performed for each sample. The average value was reported.

2.3.2 WATER VAPOR TRANSMISSION RATE (WVTR)

The WVTR of the ZnO knitted fabrics was evaluated following ASTM E96. Fabric samples were sealed on the mouth of glass bottles containing a fixed amount of water and placed inside a controlled test chamber at 25 °C and 30–35% relative humidity. The initial weight of each sample bottle (glass + water + fabric) was recorded as W_0 using a precision balance. The bottles were then reweighed (W_t) after exposure periods of 1, 2, 4, 8, 16, and 24 hours.

The WVTR was calculated using Equation (1):

$$(\text{water vapor transmission rate}) = \frac{W_0 - W_t}{A \times t} \times 100\% \dots (1)$$

Where W_0 is the initial sample weight (g), W_t is the weight after exposure (g), A is the surface area of the fabric (m^2), and t is the evaporation time (h).

2.3.3 AIR PERMEABILITY

Air permeability testing was conducted according to ASTM D737 using an air permeability tester (Model FX 3300, Textest AG, Germany). Each ZnO knitted fabric specimen measured 25 cm × 25 cm, and twelve readings were taken per sample. The average value was reported.

2.3.4 UV–VISIBLE SPECTROPHOTOMETER (OD₆₀₀) ANTIBACTERIAL TEST

For optical density analysis, 1 mL of *S. aureus* bacterial suspension (10^5 CFU/mL) was dropped onto each ZnO knitted fabric sample and incubated for 16 hours at 37 °C. After incubation, 9 mL of nutrient solution was added to each sample bottle, followed by shaking for 5 minutes. Subsequently, 1 mL of the nutrient solution was transferred into a cuvette and analyzed using a UV–visible spectrophotometer at a wavelength of 600 nm. The absorbance values were recorded, and the average was calculated.

2.3.5 ANTIBACTERIAL TEST

The antibacterial performance was evaluated according to the AATCC 100-2004 standard. Each sample was placed in a 25 mL bottle, and 1 mL of *S. aureus* bacterial suspension (10^5 CFU/mL) was added to the fabric surface, followed by incubation for 16 hours. Then, 9 mL of nutrient solution was added, and the bottles were shaken for 5 minutes. A 100 μ L aliquot of the resulting solution was spread evenly on solid nutrient agar plates, which were incubated overnight. The control group consisted of untwisted fabrics (samples 2Zn-0C-K and 3Zn-0C-K).

The antibacterial rate (R) was calculated using Equation (2):

$$R\% = \frac{A - B}{A} \times 100\% \dots \dots (2)$$

Where A is the colony count of the control (untwisted fabric, 2Zn-0C-K or 3Zn-0C-K) and B is the colony count of the test sample.

3. RESULTS AND DISCUSSION

3.1 HAIRINESS AND SURFACE MORPHOLOGY OF NANO-ZNO YARNS WITH DIFFERENT PLY NUMBERS AND TWIST COEFFICIENTS

Figure 2 presents the hairiness data of nano-ZnO yarns with varying ply numbers and twist coefficients. After twisting with a rotor spinning device, the number of hairiness per unit length decreased as the twist coefficient increased. This reduction is attributed to the enhanced inter-fiber cohesion caused by higher twist levels, which tightly bind the fibers together, resulting in fewer and shorter protruding fiber ends.

As shown in Figures 3(a)–(f), the surface morphology of three-ply nano-ZnO yarns varied significantly with twist level. Figure 3(a) shows the untwisted yarns, while Figures 3(b)–(f) display yarns twisted at twist coefficients of 1 to 5. With increasing rotor speed, the number of turns per unit length clearly increased, and the amount of hairiness visibly decreased. In particular, long hairs exceeding 3 mm were greatly reduced, leading to denser and more uniform yarns with improved overall quality[23], [24].

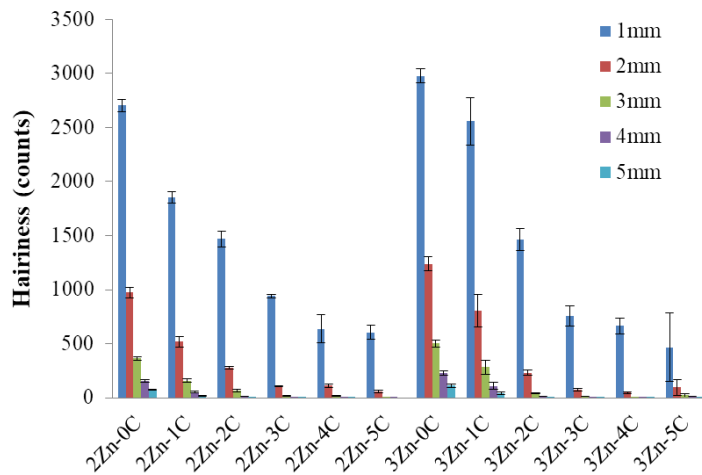


Figure 2. Hairiness of nano-ZnO yarns with different ply numbers and twist coefficients.

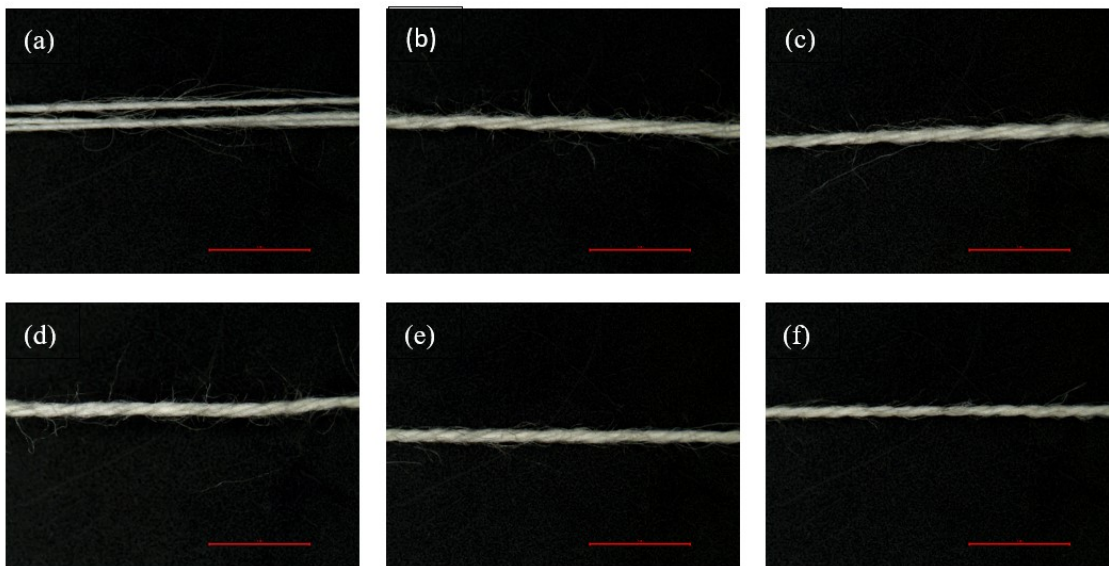


Figure 3. Schematic illustration of three-ply nano-ZnO yarns with different twist coefficients: (a) 3Zn-0C, (b) 3Zn-1C, (c) 3Zn-2C, (d) 3Zn-3C, (e) 3Zn-4C, and (f) 3Zn-5C.

3.2 EFFECT OF PLY NUMBER AND TWIST COEFFICIENT ON THE TENSILE STRENGTH OF NANO-ZNO KNITTED FABRICS

Figure 4 shows the tensile strength results of nano-ZnO knitted fabrics prepared from yarns with different ply numbers and twist coefficients using a rotor twisting machine. The data indicate that twisting significantly enhanced tensile strength due to the increased inter-fiber cohesion within the yarns. As the twist coefficient increased, the tensile strength exhibited an overall upward trend. However, for both two-ply and three-ply yarns, a noticeable decrease in strength occurred at a twist coefficient of 4. This reduction may be attributed to over-twisting, which causes partial fiber damage or breakage, thereby lowering the measured strength during tensile testing.

Additionally, the data reveal that the warp direction exhibited higher tensile strength than the weft direction. This difference arises because, under warp-direction stretching, the load is primarily borne by two loop columns per course, whereas under weft-direction stretching, it is mainly supported by a single loop arc per wale. Consequently, the smaller number of load-bearing yarns in the weft direction results in lower tensile strength compared with the warp direction [21], [25], [26].

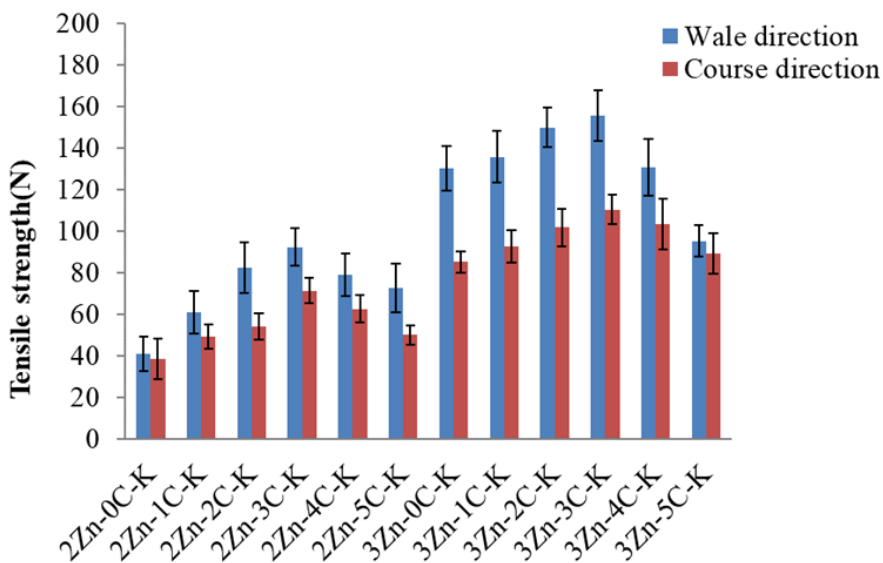


Figure 4. Tensile strength of nano-ZnO knitted fabrics with different ply numbers and twist coefficients.

3.3 EFFECT OF TWIST COEFFICIENT ON THE WATER VAPOR TRANSMISSION RATE (WVTR) OF NANO-ZNO KNITTED FABRICS

This study examined the influence of different twist coefficients on the water vapor transmission rate (WVTR) of nano-ZnO knitted fabrics. According to previous literature, the normal water vapor transmission rate of the human skin ranges from 215 to 350 g/m²/day. Therefore, when the WVTR of a fabric falls below this range, moisture condensation may occur within the fabric, leading to discomfort[27]. Factors such as fiber type, twist coefficient, fabric thickness, and fabric structure are known to significantly affect the permeability of water vapor through textiles [28], [29].

As shown in Figure 5, both two-ply and three-ply nano-ZnO knitted fabrics exhibited increasing WVTR with prolonged testing time. However, a clear downward trend in WVTR was observed with increasing twist coefficient. This phenomenon can be explained by structural compactness: fabrics made from untwisted yarns contain looser inter-yarn spaces that facilitate rapid moisture diffusion and evaporation, resulting in higher WVTR. In contrast, as the degree of twist increases, the fibers become more tightly packed, reducing pore size and hindering vapor transmission. Consequently, the WVTR decreases with higher twist coefficients[30].

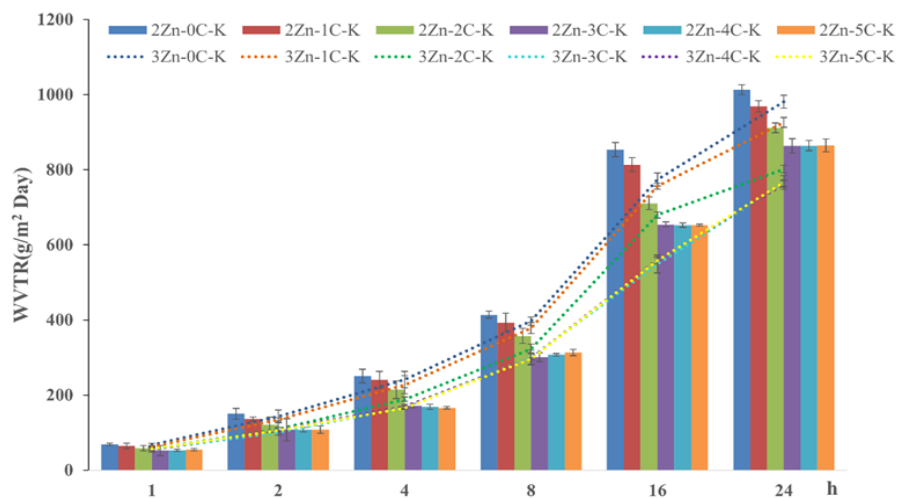


Figure 5. Water vapor transmission rate (WVTR) analysis of nano-ZnO knitted fabrics with different twist coefficients.

3.4 EFFECT OF TWIST COEFFICIENT ON THE AIR PERMEABILITY OF NANO-ZNO KNITTED FABRICS

Figure 6 shows the air permeability of nano-ZnO knitted fabrics produced from two-ply and three-ply ZnO yarns. The overall air permeability ranged from 195–271 cm³/cm²/s for two-ply fabrics and 148–194 cm³/cm²/s for three-ply fabrics. The results indicate that air permeability initially increased with increasing twist coefficient. This improvement can be attributed to enhanced fiber cohesion and tighter inter-yarn winding forces as the twist level increased, which optimized the yarn packing and allowed better air passage.

For both yarn types, the maximum air permeability was observed at a twist coefficient of 3, reaching 271 cm³/cm²/s for sample 2Zn-3C-K and 194 cm³/cm²/s for sample 3Zn-3C-K. Beyond this point, air permeability decreased with further increases in twist coefficient. This decline is explained by excessive wrapping within the same unit length, which increases fabric density and reduces porosity, thereby restricting airflow through the knitted structure [31].

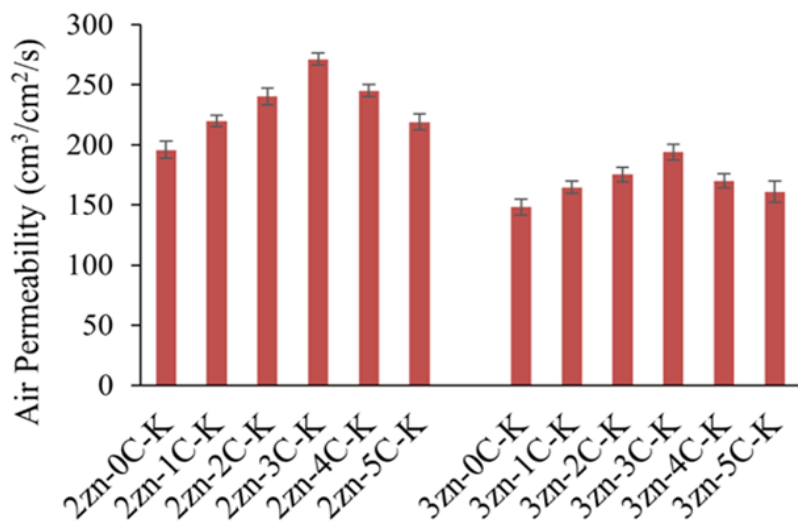


Figure 6. Air permeability analysis of nano-ZnO knitted fabrics with different twist coefficients.

3.5 ANTIBACTERIAL EFFECT OF NANO-ZNO KNITTED FABRICS WITH DIFFERENT TWIST COEFFICIENTS ANALYZED BY UV-VISIBLE SPECTROPHOTOMETRY

As shown in Figure 7, the optical density (OD) value of sample 2Zn-0C-K was 1.29, which decreased to 0.38 for 2Zn-5C-K. Similarly, the OD value of 3Zn-0C-K was 1.01, dropping to 0.21 for 3Zn-5C-K. For both two-ply and three-ply nano-ZnO knitted fabrics, the OD values exhibited a decreasing trend with increasing twist coefficient, indicating that the antibacterial activity against *Staphylococcus aureus* was enhanced.

During bacterial (*S. aureus*) growth in nutrient solution, the microorganisms consume glucose as an energy source. Through metabolic activity, acids are subsequently produced, and changes in these quantities can serve as indicators of bacterial growth. After a certain incubation period, the reduction in glucose content or the increase in metabolic acids reflects the extent of bacterial proliferation[32], [33]. However, this is only an indirect measurement, which cannot determine the total viable count precisely; it merely provides a qualitative reference for the presence or absence of antibacterial activity.

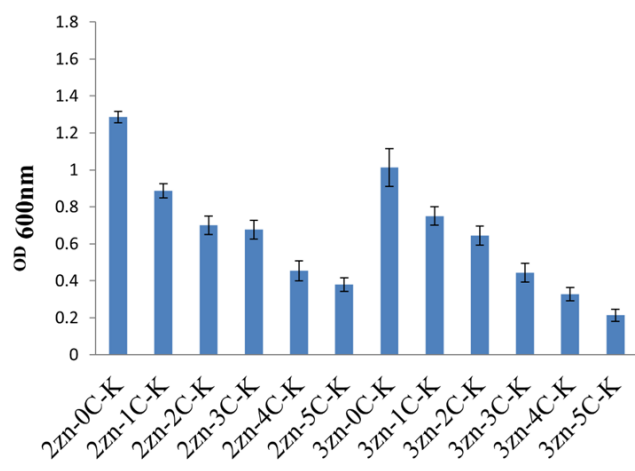


Figure 7. OD₆₀₀ antibacterial analysis of nano-ZnO knitted fabrics with different twist coefficients.

3.6 ANTIBACTERIAL EFFECT OF NANO-ZNO KNITTED FABRICS WITH DIFFERENT TWIST COEFFICIENTS AGAINST *STAPHYLOCOCCUS AUREUS*

Figures 8 and 9 show the colony growth of *S. aureus* on nano-ZnO knitted fabrics made from two-ply and three-ply yarns with different twist coefficients, respectively. Figures 8(a) and 9(a) represent the untwisted fabrics, where the bacterial colonies are dense and abundant. As the twist coefficient increased from 1 to 5, the number of colonies gradually decreased. This result suggests that a higher twist coefficient enhances the antibacterial effect, likely because a greater amount of nano-ZnO is distributed and exposed per unit area of fabric, improving bacterial inhibition.

Figure 10 shows the antibacterial rates calculated using Equation (2) for both untwisted and twisted nano-ZnO knitted fabrics. For fabrics made from two-ply yarns, the antibacterial rate increased from 33% (2Zn-1C-K) to 87% (2Zn-5C-K). For three-ply yarns, the antibacterial rate improved from 34% (3Zn-1C-K) to 90% (3Zn-5C-K). These findings demonstrate that both increasing the ply number and twist coefficient enhance antibacterial performance. The improvement is attributed to a higher concentration of nano-ZnO on the fabric surface within the same area, which strengthens the antimicrobial activity.

The antibacterial activity of nano-ZnO against *S. aureus* can be explained by its physicochemical interactions and photocatalytic effects. *S. aureus* is a Gram-positive bacterium with a phospholipid-based inner lipid layer carrying a negatively charged surface, primarily due to carboxyl (–COOH) and other functional groups on its cell wall and membrane. When ZnO nanoparticles (ZnO NPs) come into contact with the bacterial surface, Zn²⁺ ions released from the particles are electrostatically attracted to the cell wall, causing initial membrane damage. The Zn²⁺ ions further interfere with peptidoglycan cross-linking and biosynthesis, weakening the structural integrity of the cell wall and inhibiting cell proliferation. Once the membrane is compromised, Zn²⁺ ions penetrate the cell and bind to intracellular proteins and nucleic acids via coordination with thiol (–SH) and amino (–NH₂) groups, leading to protein denaturation, enzyme deactivation, and leakage of intracellular contents.

In addition, several studies have reported that under visible light irradiation, ZnO nanoparticles exhibit photocatalytic activity, generating electron–hole pairs (e^-/h^+). These charged species react with water and oxygen to form highly reactive reactive oxygen species (ROS), such as hydroxyl radicals ($\cdot OH$) and superoxide anions ($O_2^{\cdot-}$). The ROS attack bacterial membranes, proteins, and DNA, inducing oxidative stress that disrupts normal cellular metabolism, growth, and reproduction processes [34], [35], [36], [37], [38].

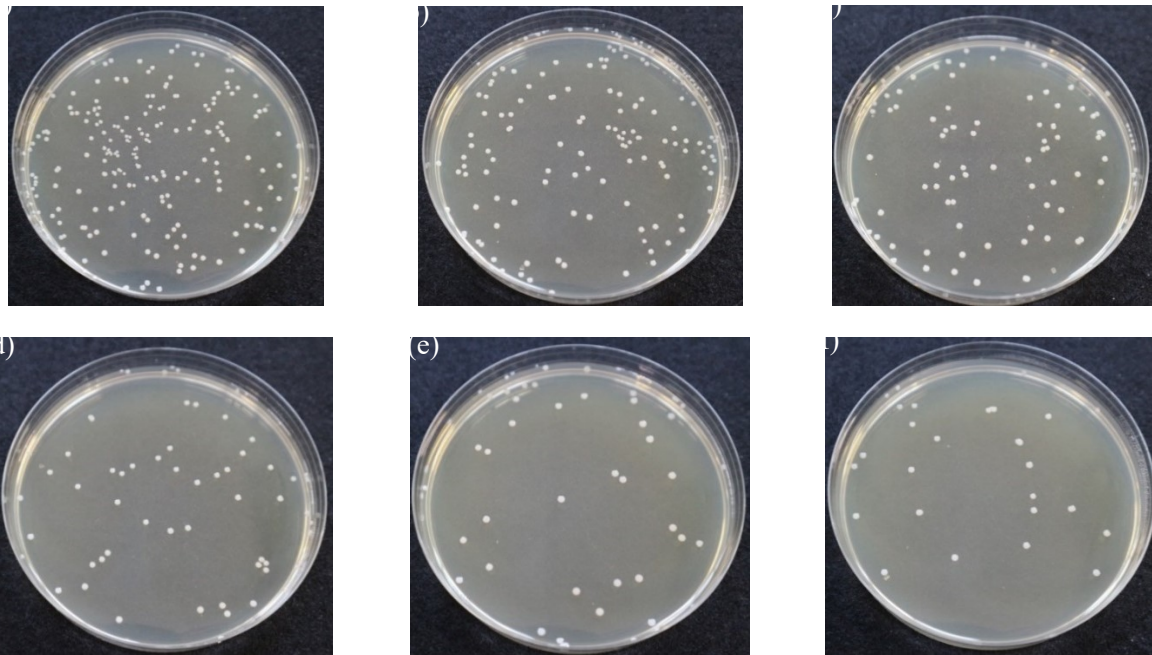


Figure 8. Photographs of *S. aureus* colonies on two-ply nano-ZnO knitted fabrics with different twist coefficients: (a) 2Zn-0C-K, (b) 2Zn-1C-K, (c) 2Zn-2C-K, (d) 2Zn-3C-K, (e) 2Zn-4C-K, and (f) 2Zn-5C-K.

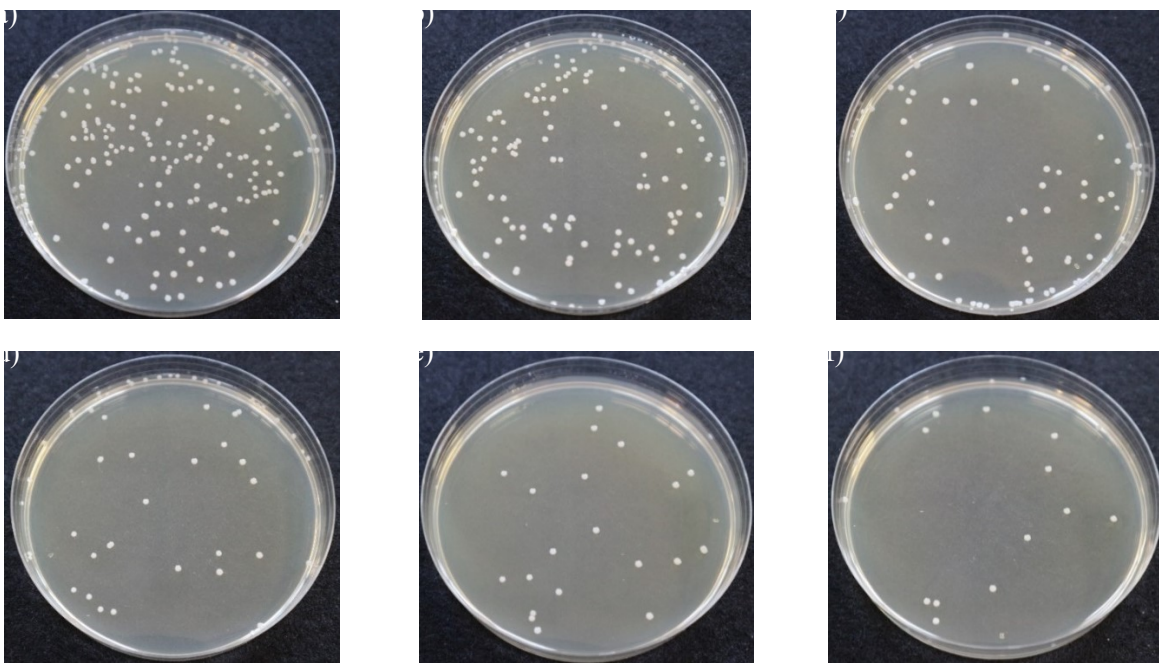


Figure 9. Photographs of *S. aureus* colonies on three-ply nano-ZnO knitted fabrics with different twist coefficients: (a) 3Zn-0C-K, (b) 3Zn-1C-K, (c) 3Zn-2C-K, (d) 3Zn-3C-K, (e) 3Zn-4C-K, and (f) 3Zn-5C-K.

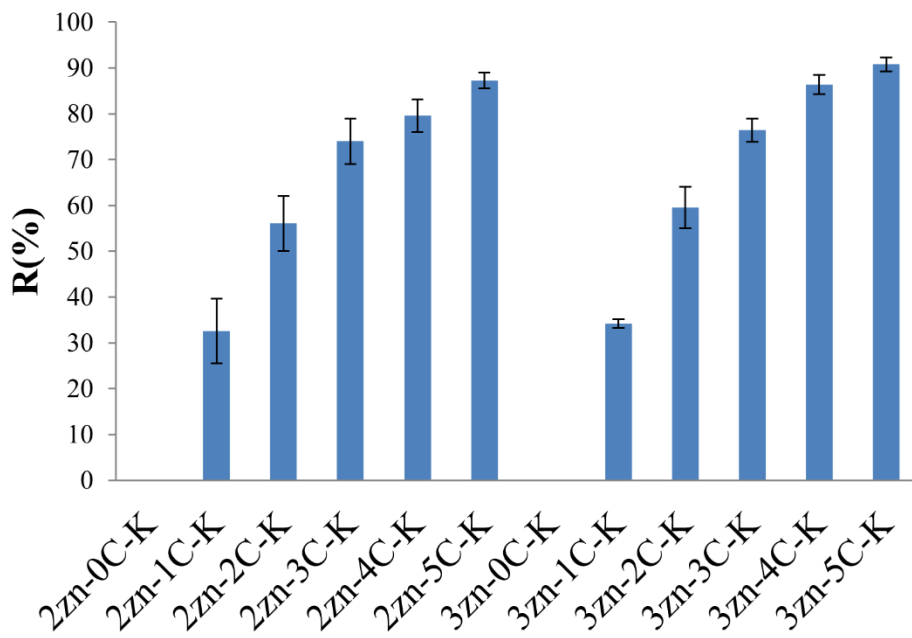


Figure 10. Antibacterial rates of nano-ZnO knitted fabrics with different twist coefficients.

4. CONCLUSION

In this study, twelve nano-ZnO knitted fabrics with different combinations of twist coefficients were successfully developed using a rotor twisting technique. The mechanical and biological performances of these fabrics were systematically evaluated. The results demonstrated that the twist coefficient is a critical processing parameter influencing both mechanical properties and antibacterial effectiveness.

From a mechanical perspective, increasing the twist coefficient reduced fiber hairiness, enhanced yarn integrity, and improved fabric compactness. The knitted fabrics 2Zn-3C-K and 3Zn-3C-K exhibited the highest tensile strength and air permeability at a twist coefficient of 3. However, when the twist coefficient exceeded 4, tensile strength decreased due to over-twisting and partial fiber breakage.

From a biological perspective, both OD₆₀₀ and colony count analyses against *Staphylococcus aureus* revealed that antibacterial performance improved with increasing twist coefficient. This enhancement may result from a more uniform distribution of nano-ZnO and a larger effective contact area with bacterial cells, promoting the generation of reactive oxygen species (ROS) and Zn²⁺ ion release. The sample 3Zn-5C-K achieved an antibacterial rate of 90%, confirming that physical encapsulation of nano-ZnO effectively strengthens bactericidal efficiency.

Overall, the samples 2Zn-3C-K and 3Zn-3C-K (twist coefficient 3) demonstrated optimal balance between mechanical strength and comfort, while 2Zn-5C-K and 3Zn-5C-K (twist coefficient 5) exhibited maximum antibacterial efficacy. Considering cost-effectiveness and process stability, the two-ply nano-ZnO yarn twisted at 15,000 rpm (sample 2Zn-5C-K) represents the most balanced and practical configuration, suitable for medical protective textiles and smart functional applications.

5. FUNDING

This research was funded by the Ministry of Science and Technology of Taiwan, grant number 114-2622-E-468 -004 and CMU111-N-08.

6. REFERENCES

1. L. Lin, C. Haiying, M. A.-S. Abdel-Samie, and G. Abdulla, '4 - Common, existing and future applications of antimicrobial textile materials', in *Antimicrobial Textiles from Natural Resources*, Md. I. H. Mondal, Ed., Woodhead Publishing, 2021, pp. 119–163. doi: 10.1016/B978-0-12-821485-5.00005-6.
2. L. Wang, D. He, L. Qian, B. He, and J. Li, 'Preparation of conductive cellulose fabrics with durable antibacterial properties and their application in wearable electrodes', *International Journal of Biological Macromolecules*, vol. 183, pp. 651–659, July 2021, doi: 10.1016/j.ijbiomac.2021.04.176.
3. G. Madhan, A. A. Begam, L. V. Varsha, R. Ranjithkumar, and D. Bharathi, 'Facile synthesis and characterization of chitosan/zinc oxide nanocomposite for enhanced antibacterial and photocatalytic activity', *International Journal of Biological Macromolecules*, vol. 190, pp. 259–269, Nov. 2021, doi: 10.1016/j.ijbiomac.2021.08.100.
4. K. Kachare et al., 'Bio-mediated synthesized zinc oxide coated on cotton fabric for antibacterial and wound healing application', *Surface and Coatings Technology*, vol. 491, p. 131171, Sept. 2024, doi: 10.1016/j.surfcoat.2024.131171.
5. M. C. Sportelli et al., 'Biogenic Synthesis of ZnO Nanoparticles and Their Application as Bioactive Agents: A Critical Overview', *Reactions*, vol. 3, no. 3, pp. 423–441, 2022, doi: 10.3390/reactions3030030.
6. B. K. Dejene, 'Biosynthesized ZnO nanoparticle-functionalized fabrics for antibacterial and biocompatibility evaluations in medical applications: A critical review', *Materials Today Chemistry*, vol. 42, p. 102421, Dec. 2024, doi: 10.1016/j.mtchem.2024.102421.
7. S. Barage et al., 'Nanomaterial in food packaging: A comprehensive review', *Journal of Nanomaterials*, vol. 2022, no. 1, p. 6053922, 2022.
8. P. Petkova, A. Francesko, I. Perelshtein, A. Gedanken, and T. Tzanov, 'Simultaneous sonochemical-enzymatic coating of medical textiles with antibacterial ZnO nanoparticles', *Ultrasonics Sonochemistry*, vol. 29, pp. 244–250, Mar. 2016, doi: 10.1016/j.ultsonch.2015.09.021.
9. S. Gharpure and B. Ankamwar, 'Synthesis and antimicrobial properties of zinc oxide nanoparticles', *Journal of Nanoscience and Nanotechnology*, vol. 20, no. 10, pp. 5977–5996, 2020.
10. S. Raha and M. Ahmaruzzaman, 'ZnO nanostructured materials and their potential applications: progress, challenges and perspectives', *Nanoscale Advances*, vol. 4, no. 8, pp. 1868–1925, 2022.
11. T. S. Roy, S. U. D. Shamim, M. K. Rahman, F. Ahmed, and M. Gafur, 'The development of ZnO nanoparticle coated cotton fabrics for antifungal and antibacterial applications', *Materials Sciences and Applications*, vol. 11, no. 9, pp. 601–610, 2020.
12. S. A. Mousa, E.-S. R. El-Sayed, S. S. Mohamed, M. A. Abo El-Seoud, A. A. Elmehlawy, and D. A. Abdou, 'Novel mycosynthesis of Co₃O₄, CuO, Fe₃O₄, NiO, and ZnO nanoparticles by the endophytic *Aspergillus terreus* and evaluation of their antioxidant and antimicrobial activities', *Applied Microbiology and Biotechnology*, vol. 105, pp. 741–753, 2021.
13. A. Arputharaj, Prasad ,Virendra, Saxena ,Sujata, Nadanathangam ,Vigneshwaran, and S. R. and Shukla, 'Ionic liquid mediated application of nano zinc oxide on cotton fabric for multi-functional properties', *The Journal of The Textile Institute*, vol. 108, no. 7, pp. 1189–1197, July 2017, doi: 10.1080/00405000.2016.1222984.
14. G. D. Patil, A. H. Patil, S. A. Jadhav, C. R. Patil, and P. S. Patil, 'A new method to prepare superhydrophobic cotton fabrics by post-coating surface modification of ZnO nanoparticles', *Materials Letters*, vol. 255, p. 126562, Nov. 2019, doi: 10.1016/j.matlet.2019.126562.
15. B. Babu et al., 'Synthesis of zinc oxide nanoparticles and its applications in the surface modification of textile materials', *Journal of Optoelectronic and Biomedical Materials*, vol. 13, pp. 171–176, Oct. 2021, doi: 10.15251/JOBM.2021.134.171.
16. O. M. Darwesh, I. A. Matter, N. G. Al-Balakoc, and M. I. Abo-Alkasem, 'Circular economy reinforcement through molecular fabrication of textile wastes with microbial synthesized ZnO nanoparticles to have multifunctional properties', *Scientific Reports*, vol. 14, no. 1, p. 16660, July 2024, doi: 10.1038/s41598-024-66430-1.
17. A. K. Mandal et al., 'Current Research on Zinc Oxide Nanoparticles: Synthesis, Characterization, and Biomedical Applications', *Nanomaterials*, vol. 12, no. 17, 2022, doi: 10.3390/nano12173066.
18. L. E. Román et al., 'Blocking erythemally weighted UV radiation using cotton fabrics functionalized with ZnO nanoparticles in situ', *Applied Surface Science*, vol. 469, pp. 204–212, Mar. 2019, doi: 10.1016/j.apsusc.2018.11.047.



19. A. Hazlehurst, M. Sumner, and M. Taylor, 'Investigating the influence of yarn characteristics on microfibre release from knitted fabrics during laundering', *Frontiers in Environmental Science*, vol. 12, p. 1340229, 2024.
20. T. Liu, K. Choi, and Y. Li, 'Wicking in twisted yarns', *Journal of Colloid and Interface Science*, vol. 318, no. 1, pp. 134–139, Feb. 2008, doi: 10.1016/j.jcis.2007.10.023.
21. U. Ahmed, T. Hussain, and S. Abid, 'Role of knitted techniques in recent developments of biomedical applications: A review', *Journal of Engineered Fibers and Fabrics*, vol. 18, p. 15589250231180293, 2023.
22. S. Kovačević and D. Ujević, '16 - Seams in car seat coverings: properties and performance', in *Joining Textiles*, I. Jones and G. K. Stylios, Eds, Woodhead Publishing, 2013, pp. 478–506. doi: 10.1533/9780857093967.4.478.
23. [B. K. Dejene and M. and Ayele, 'Impact of Weft Yarn Structure and Fiber Type on Weft Yarn Velocity and Twist Loss in Air-Jet Weaving: A Critical Review', *Journal of Natural Fibers*, vol. 21, no. 1, p. 2365961, Dec. 2024, doi: 10.1080/15440478.2024.2365961.
24. A. Admas and M. Ayele, 'Impacts of yarn hairiness and voluminous on weft yarn speed and twist loss in air-jet weaving', *Journal of Natural Fibers*, vol. 20, no. 2, p. 2253372, 2023.
25. D. J. Spencer, *Knitting technology: a comprehensive handbook and practical guide*, vol. 16. CRC press, 2001.
26. R. Fangueiro and F. Soutinho, 'Textile structures', in *Fibrous and composite materials for civil engineering applications*, Elsevier, 2011, pp. 62–91.
27. G. C. Türkoğlu, A. M. Sarışık, and S. Y. Karavana, 'Development of textile-based sodium alginate and chitosan hydrogel dressings', *International Journal of Polymeric Materials and Polymeric Biomaterials*, vol. 70, no. 13, pp. 916–925, 2021.
28. E. Kamalha, Y. Zeng, J. I. Mwasiagi, and S. Kyatuheire, 'The comfort dimension; a review of perception in clothing', *Journal of sensory studies*, vol. 28, no. 6, pp. 423–444, 2013.
29. A. Majumdar, S. Mukhopadhyay, and R. Yadav, 'Thermal properties of knitted fabrics made from cotton and regenerated bamboo cellulosic fibres', *International Journal of Thermal Sciences*, vol. 49, no. 10, pp. 2042–2048, 2010.
30. S. F. Kabir, I. Uluturk, R. Pang, N. Khadse, S. E. Stapleton, and J. H. Park, 'Structure–property investigation of knit patterns on thermal comfort: A holistic approach', *ACS Applied Engineering Materials*, vol. 1, no. 5, pp. 1455–1466, 2023.
31. S. Ghayempour and M. Montazer, 'Ultrasound irradiation based in-situ synthesis of star-like Tragacanth gum/zinc oxide nanoparticles on cotton fabric', *Ultrasonics sonochemistry*, vol. 34, pp. 458–465, 2017.
32. V. C. Thomas, S. S. Chaudhari, J. Jones, M. C. Zimmerman, and K. W. Bayles, 'Electron paramagnetic resonance (EPR) spectroscopy to detect reactive oxygen species in *Staphylococcus aureus*', *Bio-protocol*, vol. 5, no. 17, pp. e1586–e1586, 2015.
33. V. C. Thomas et al., 'A central role for carbon-overflow pathways in the modulation of bacterial cell death', *PLoS pathogens*, vol. 10, no. 6, p. e1004205, 2014.
34. P. Nikolic, P. Mudgil, D. G. Harman, and J. Whitehall, 'Untargeted lipidomic differences between clinical strains of methicillin-sensitive and methicillin-resistant *Staphylococcus aureus*', *Infectious Diseases*, vol. 54, no. 7, pp. 497–507, 2022.
35. M. Premanathan, K. Karthikeyan, K. Jeyasubramanian, and G. Manivannan, 'Selective toxicity of ZnO nanoparticles toward Gram-positive bacteria and cancer cells by apoptosis through lipid peroxidation', *Nanomedicine: Nanotechnology, Biology and Medicine*, vol. 7, no. 2, pp. 184–192, 2011.
36. M. Du et al., 'Visible-light-driven photocatalytic inactivation of *S. aureus* in aqueous environment by hydrophilic zinc oxide (ZnO) nanoparticles based on the interfacial electron transfer in *S. aureus*/ZnO composites', *Journal of Hazardous Materials*, vol. 418, p. 126013, 2021.
37. I. Nasim et al., 'Green synthesis of ZnO nanoparticles and biological applications as broad-spectrum bactericidal, antibiofilm effects and biocompatibility studies on Zebrafish embryo', *Inorganic Chemistry Communications*, vol. 169, p. 113049, 2024.
38. E. Hoseinzadeh, M.-Y. Alikhani, M.-R. Samarghandi, and M. Shirzad-Siboni, 'Antimicrobial potential of synthesized zinc oxide nanoparticles against gram positive and gram negative bacteria', *Desalination and Water Treatment*, vol. 52, no. 25–27, pp. 4969–4976, 2014.